Acta Scientiarum
http://periodicos.uem.br/ojs
ISSN on-line: 1807-8664
https://doi.org/10.4025/actascitechnol.v48i1.74255

Theoretical framework for DOUBLE-DOUBLE composite plates under bending loads

Tiago Teixeira Silva[1], Nathalia Mello Mascarenhas Paixão[2], Hélio de Assis Pegado[1*] and Antonio Ferreira Ávila[1]

[1]Programa de Pós-Graduação em Engenharia Mecânica, Universidade Federal de Minas Gerais, Avenida Antônio Carlos, 6627, Pampulha, 31270-901, Belo Horizonte, Minas Gerais, Brasil. [2]Departamento de Engenharia Mecânica, Centro Federal de Educação Tecnológica de Minas Gerais, Belo Horizonte, Minas Gerais, Brasil. *Author for correspondence. E-mail: helio@demec.ufmg.br

ABSTRACT. This paper provides an insightful comparative analysis of laminated composite plates, focusing on two main stacking sequence groups: the traditional QUAD and the more recent DOUBLE-DOUBLE (DD) proposed by Professor Stephen Tsai. The investigation thoroughly explores the extensional, coupling, and bending stiffness matrices of each group, analyzing their implications for the bending behavior of laminated composite plates according to Kirchhoff's Laminate Theory under cylindrical bending conditions. The study highlights that, under this theory, increasing the repetitions of the 4-layer sub-laminates [±Φ/±ψ] leads to a much greater increase in bending than in coupling stiffness, and simultaneously promotes a decrease in extension-bending (A_{16}, A_{26}) and bending-torsion (D_{16}, D_{26}) components. The finite element simulations indicate that, as the number of repetitions increases from two to eight, the reduction in out-of-plane displacement exceeds that of the corresponding QUAD configuration, making the DD configuration a promising option. Moreover, the choice of angles significantly influences the overall bending behavior, particularly affecting three key components of the bending stiffness matrix: D_{11}, D_{16}, and D_{26}. Among the configurations examined, the $[\pm 0/\pm 50]_8$ configuration emerges as the optimal DD configuration for bending applications. This specific angle combination for the [± 0/± 50] sub-laminate yields high values of D_{11} and near-zero values for D_{16} and D_{26}, enhancing bending stiffness while minimizing coupling twist-bending. In conclusion, the findings suggest that DD configurations offer a valuable option for applications involving thick composite bending.

Keywords: Double-double; QUAD; Kirchhoff's laminate theory; numerical simulations.

Received on May 07, 2025.
Accepted on June 16, 2025.

Introduction

Since the 1960 s, when the aeronautical industry began using composite materials, the QUAD stacking sequence has been continuously employed (Vermes et al., 2021a). QUAD laminates utilize 0°, ± 45°, and 90° angular layer orientations, with symmetry conditions and adherence to the 10 percent rule (Hart-Smith, 2004). The 10 percent rule, proposed by Hart-Smith, offers a simplified method for determining the stiffness and mechanical strength of laminated composites. It suggests that the stiffness of the ± 45° and 90° layers should be considered as 10% of the stiffness and/or strength of the 0° layers. The various permutations of these three basic orientations, along with the straightforward calculation method and the satisfactory results obtained, have led the composites industry to adopt the QUAD configuration as a standard.

Recently, Professor Stephen Tsai introduced a new stacking sequence, based on the continuous repetition of a 4-layer sub-laminate in the form of [±Φ/±ψ], termed double-double (DD) (Tsai, 2021). The proposed DD configuration is grounded in the principle of Tsai's modulus, which is an invariant quantity (Arteiro et al., 2020). According to Vermes et al., the DD configuration offers several advantages over the traditional QUAD configuration (Vermes et al., 2021b). One such advantage is ease of manufacturing, as simply repeating the sub-laminate is much faster, potentially reducing production costs. Additionally, Wang et al. (2023) note that, besides ease of manufacturing, the DD configuration can yield lighter-weight laminates with equivalent stiffness and mechanical strength compared to the QUAD configuration. However, Zhao et al. (2023) suggest that utilizing the DD configuration results in an unsymmetrical laminate. It is important to note that in an unsymmetrical laminate, consideration of the coupling matrix is necessary to prevent warping (Patton et al.,

2021). The issue of extension-flexion-torsion coupling can be addressed by increasing the number of sub-laminate repetitions, thereby reducing the coupling matrix [B] to values approaching zero (Shrivastava et al., 2020).

Studies by Vermes et al. (2021b) and Zhang et al. (2022) demonstrate that the DD configuration yields similar outcomes to QUAD configurations for open-hole laminate problems under tensile (OHT) and compressive (OHC) stresses. However, the behavior of stress and strain fields in DD laminates under bending remains an open question.

This paper aims to examine the effects of various DD configurations compared to QUAD configurations on the stiffness matrices for extension, coupling, and bending under the Classical Laminated Plate Theory (CLPT) point of view. Additionally, it seeks to explore how stacking sequences influence the stress and strain fields of laminated beams subjected to bending loads. To accomplish the primary objective of this research, MATLAB was employed as the primary tool.

Materials and methods

In this study, certain fundamental conditions for computational modeling are taken into account. Unlike the approach adopted by Carley et al. (2013), the interactions between the interfaces of the layers are neglected, implying an assumption of perfect interface conditions. This condition also presupposes the absence of porosity (Ávila & Morais, 2009). Given that the objective of this work is to 'map' the distribution of stress and strain fields in laminated composite plates, the analysis will be confined to the elastic region (Ávila & Tamma, 1998).

The comparative analysis of the stiffness matrices relies on Kirchhoff's Laminate Theory (Maji & Mahato, 2022). The stress-strain relationships for each m^{th} layer of the laminate are delineated in (Equation 1).

$$\begin{bmatrix}\sigma_x\\ \sigma_y\\ \tau_{xy}\end{bmatrix}_m = \begin{bmatrix}\overline{Q}_{11} & \overline{Q}_{12} & \overline{Q}_{16}\\ \overline{Q}_{12} & \overline{Q}_{22} & \overline{Q}_{26}\\ \overline{Q}_{16} & \overline{Q}_{26} & \overline{Q}_{66}\end{bmatrix}_m \begin{bmatrix}\varepsilon_x^o & \kappa_x\\ \varepsilon_y^o & + \kappa_y\\ \gamma_{xy}^o & \kappa_{xy}\end{bmatrix}_m \tag{1}$$

Indeed, in accordance with Kirchhoff's theory, the stress vector is represented by two normal stresses (σ_x and σ_y) and a shear stress (τ_{xy}). The reduced stiffness matrix ($\overline{Q_{ij}}$) follows the procedure outlined by other authors (Paixão & Ávila, 2023). The total deformation can be partitioned into the vector of deformations in the median plane ($\varepsilon_x^o, \varepsilon_y^o, \gamma_{xy}^o$) and the curvature vector ($\kappa_x, \kappa_y, \kappa_{xy}$) (Sheikhi et al., 2024).

The constitutive relations for laminates remain independent of their configuration, whether QUAD or DD. (Equations 2) and (Equations 3) delineate the forces and moments acting on the laminate as a function of the reduced stiffness matrix and the total deformation (Yu, 2024).

$$\begin{bmatrix}N_x\\ N_y\\ N_{xy}\end{bmatrix} = \sum_{m=1}^{n} \begin{bmatrix}\overline{Q}_{11} & \overline{Q}_{12} & \overline{Q}_{16}\\ \overline{Q}_{12} & \overline{Q}_{22} & \overline{Q}_{26}\\ \overline{Q}_{16} & \overline{Q}_{26} & \overline{Q}_{66}\end{bmatrix}_m \left[\int_{z_{m-1}}^{z_m} \begin{bmatrix}\varepsilon_x^o\\ \varepsilon_y^o\\ \gamma_{xy}^o\end{bmatrix} dz + \int_{z_{m-1}}^{z_m} \begin{bmatrix}\kappa_x\\ \kappa_y\\ \kappa_{xy}\end{bmatrix} z dz\right] \tag{2}$$

$$\begin{bmatrix}M_x\\ M_y\\ M_{xy}\end{bmatrix} = \sum_{m=1}^{n} \begin{bmatrix}\overline{Q}_{11} & \overline{Q}_{12} & \overline{Q}_{16}\\ \overline{Q}_{12} & \overline{Q}_{22} & \overline{Q}_{26}\\ \overline{Q}_{16} & \overline{Q}_{26} & \overline{Q}_{66}\end{bmatrix}_m \left[\int_{z_{m-1}}^{z_m} \begin{bmatrix}\varepsilon_x^o\\ \varepsilon_y^o\\ \gamma_{xy}^o\end{bmatrix} z dz + \int_{z_{m-1}}^{z_m} \begin{bmatrix}\kappa_x\\ \kappa_y\\ \kappa_{xy}\end{bmatrix} z^2 dz\right] \tag{3}$$

The explicit forms of (Equation 2) and (Equation 3) can be written as:

$$\begin{bmatrix}N_x\\ N_y\\ N_{xy}\end{bmatrix} = \begin{bmatrix}A_{11} & A_{12} & A_{16}\\ A_{12} & A_{22} & A_{26}\\ A_{16} & A_{26} & A_{66}\end{bmatrix} \begin{bmatrix}\varepsilon_x^o\\ \varepsilon_y^o\\ \gamma_{xy}^o\end{bmatrix} + \begin{bmatrix}B_{11} & B_{12} & B_{16}\\ B_{12} & B_{22} & B_{26}\\ B_{16} & B_{26} & B_{66}\end{bmatrix} \begin{bmatrix}\kappa_x\\ \kappa_y\\ \kappa_{xy}\end{bmatrix} \tag{4}$$

$$\begin{bmatrix}M_x\\ M_y\\ M_{xy}\end{bmatrix} = \begin{bmatrix}B_{11} & B_{12} & B_{16}\\ B_{12} & B_{22} & B_{26}\\ B_{16} & B_{26} & B_{66}\end{bmatrix} \begin{bmatrix}\varepsilon_x^o\\ \varepsilon_y^o\\ \gamma_{xy}^o\end{bmatrix} + \begin{bmatrix}D_{11} & D_{12} & D_{16}\\ D_{12} & D_{22} & D_{26}\\ D_{16} & D_{26} & D_{66}\end{bmatrix} \begin{bmatrix}\kappa_x\\ \kappa_y\\ \kappa_{xy}\end{bmatrix} \tag{5}$$

where [A] represents the extensional stiffness matrix, [B] characterizes the coupling stiffness matrix, while [D] describes the bending stiffness matrix, and N and M represent the forces and moments per unit length.

The mathematical expressions for calculating each of the stiffness matrices (Mantzaroudis & Stamatelos, 2020) are reproduced in (Equation 6), (Equation 7), and (Equation 8).

$$A_{ij} = \sum_{m=1}^{n} \left(\overline{Q}_{ij}\right)_m (z_m - z_{m-1}) \tag{6}$$

$$B_{ij} = \frac{1}{2}\sum_{m=1}^{n} \left(\overline{Q}_{ij}\right)_m (z_m^2 - z_{m-1}^2) \tag{7}$$

$$D_{ij} = \frac{1}{3}\sum_{m=1}^{n} \left(\overline{Q}_{ij}\right)_m (z_m^3 - z_{m-1}^3) \tag{8}$$

The equilibrium (Equation 9), (Equation 10) for composite plates can be described using the following expressions (Kollar & Springer, 2003):

$$\frac{\partial N_x}{\partial x} + \frac{\partial N_{xy}}{\partial y} = -p_x, \frac{\partial N_y}{\partial y} + \frac{\partial N_{xy}}{\partial x} = -p_y, \frac{\partial V_x}{\partial x} + \frac{\partial V_y}{\partial y} = -p_z \tag{9}$$

$$V_x = \frac{\partial M_x}{\partial x} + \frac{\partial M_{xy}}{\partial y}, V_y = \frac{\partial M_y}{\partial y} + \frac{\partial M_{xy}}{\partial x} \tag{10}$$

Indeed, in the given study, p_x, p_y, and p_z represent the components of the load distributed on the surface per unit area. N_x, N_y, and N_{xy} denote the in-plane forces per unit length, while V_x and V_y represent the transverse shear forces per unit length.

The analysis undertaken considers the deflection condition of rectangular composite plates subjected to pure bending and loads acting in the plane. It is feasible to compute the deflection if the curvatures are known, simply by solving (Equation 4) and (Equation 5).

The equation that 'maps' the deflection (w) in a rectangular composite plate can be described as a function of the curvatures:

$$w = \frac{-\kappa_x}{2}x^2 - \frac{\kappa_y}{2}y^2 - \frac{\kappa_{xy}}{2}xy \tag{11}$$

Since this study assumes the long plate condition, the cylindrical bending condition in the x direction can be adopted. It is crucial to note that, in this study, the long plate cylindrical bending condition implies the zero curvature condition for κ_y and κ_{xy}, and all derivatives with respect to the y-axis are equal to zero (Kollar & Springer, 2003). This condition implies that away from the shorter sides, the forces and moments do not vary along the length of the plate. Consequently, it is possible to rewrite (Equation 9) and (Equation 10) as:

$$\frac{dV_x}{dx} + p_z = 0, \tag{12}$$

$$\frac{dM_x}{dx} - V_x = 0 \tag{13}$$

As the load p_z is perpendicular to the surface, it is possible to replace p_z with p in (Equation 12), and replacing V_x from (Equation 13) into (Equation 12) gives,

$$\frac{d^2M_x}{dx^2} + p = 0 \tag{14}$$

It is worth noting that (Equation 14) represents equilibrium, and it is independent of the material. For a symmetrical laminate ([B]= 0), such as in the case of QUADs, (Equation 5) is described as:

$$M_x = D_{11}\kappa_x \tag{15}$$

By replacing (Equation 15) with (Equation 14) and considering the definition of curvature (κ_x), it is possible to establish an equation similar to that describing the displacement of an isotropic beam with transverse loading. Consequently, the equilibrium equation of a long plate for a symmetrical composite with QUAD-type laminates can be expressed as:

$$\frac{d^4w}{dx^4} - \frac{p}{D_{11}} = 0 \tag{16}$$

The analysis of DD laminates is more intricate, as they are unsymmetrical, resulting in [B] $\neq$ 0. In the scenario of unsymmetrical laminates, it is essential to enforce a displacement restriction on one of the sides in the direction of the 'longest side' (y-direction). This restriction ensures that the longitudinal deformation in the y-direction is zero across the entire plate (Singh & Kumari, 2020). Another critical condition is that the

shear force (N_{xy}) is zero. An approximation to achieve the true zero shear condition is to restrain (by clamping or providing simple support) the two long sides (Falkowicz, 2021).

Deflections and maximum bending moments of unsymmetric plates can be approximated by replacing the bending stiffness matrix with a reduced bending stiffness matrix (Whitney,1987):

$$\left[D\ \right] = [D] - [B][A]^{-1}[B] \tag{17}$$

Moreover, this 'reduced' bending stiffness matrix allow us to use all equations developed for bending symmetric laminates with loss of generality (O'Donnell & Weaver, 2020).

The equations provided describe the transverse displacements (w) for both QUAD and DD laminates under the cylindrical bending condition. One last crucial piece of information is that for the long plate condition to be satisfied for an orthotropic laminate, whether QUAD or DD, the following inequality must be true (Kollar & Springer, 2003):

$$\frac{L_y}{L_x} > \sqrt[4]{\frac{D_{11}}{D_{22}}} \tag{18}$$

where Lx and Ly are the plate length and width, respectively.

The numerical simulations were carried out using MATLAB 2023 and the finite element method using ANSYS 2023R1. The cases studied, with their respective mechanical properties, are listed in Table 1. The stacking sequences represent some of the cases listed in other studies (Tsai, 2021; Vermes et al., 2021b). The idea behind this study is to understand how the number of repetitions and fiber orientations can influence the laminate's overall response to bending loads.

Table 1. Stacking sequence and mechanical properties.

Case	QUAD	DOUBLE-DOUBLE			Plies
1	$[0/\pm 45/ 90]_S$	$[\pm 18/\pm 62]_2$	$[\pm 0/\pm 50]_2$	$[\pm 22.5/\pm 52.5]_2$	8
2	$[0_3/\pm 45_2/ 90]_S$	$[\pm 18/\pm 62]_4$	$[\pm 0/\pm 50]_4$	$[\pm 22.5/\pm 52.5]_4$	16
3	$[0/\pm 45/ 90]_{4S}$	$[\pm 18/\pm 62]_8$	$[\pm 0/\pm 50]_8$	$[\pm 22.5/\pm 52.5]_8$	32
Mechanical properties for UD carbon fiber/epoxy composite E_1 = 121.0 GPa, $E_2 = E_3$ = 8.60 GPa, $G_{12} = G_{13}$ = 4.70 GPa, G_{23} = 3.1 GPa, $\nu_{12} = \nu_{13}$ = 0.27, ν_{23} = 0.40 Ply thickness = 0.125 mm					

Results and discussion

This study is divided into two parts: the first part focuses on the analysis of the stiffness matrices (extensional, coupling, and bending), while the second part focuses on computational modeling of laminated plates under cylindrical bending conditions (Nimbolkar & Jain, 2015). For the DD configuration, the coupling problem is mitigated by repeating the sub-laminates, aiming to minimize the warping of the laminate (Vermes et al., 2021b). However, warping arises from the coupling between in-plane and out-of-plane deformations ($B_{11}\neq 0$, $B_{12}\neq 0$, and $B_{66}\neq 0$). It is worth mentioning that when $B_{16}\neq 0$, there is extension-torsion coupling. These couplings persist until the coupling stiffness matrix is identically equal to zero, i.e., [B] = 0 (Whitney, 1987).

Table 2 shows a comparative study between QUAD and DD considering the stiffness matrices. As anticipated, the coupling stiffness matrices, [B], for symmetrical laminates are indeed zero refer to Table 2. It is worth noting that values of B_{ij} less than or equal to 1.0×10^{-8} were considered as null. For the DD laminates, under the CLPT, the coupling effect is still present. The argument put forth by Vermes et al. (2021a), suggesting that coupling/shrinkage is reduced with an increase in sub-laminate repetitions, is grounded on the premise that the stiffness matrices should be normalized by the Tsai modulus (Melo et al., 2017). This approach decreases the three stiffness matrices (extensional, coupling, and bending), minimizing out-of-plane deformations (warping). From the CLPT point of view, the analysis is different. The increase in repetitions has a direct effect on the extension-shear coupling, as A_{16} and A_{26} make it close to zero. Additionally, the bending-torsion coupling (D_{16} and D_{26}) for DD laminates has been mitigated. These effects must be added to the increase in bending components, more specifically D_{11}, D_{22}, D_{12}, and D_{66}. For the cases studied, these values increased by one order of magnitude when the thickness doubled. At the same time, the in-plane and out-of-plane coupling components, i.e., B_{11}, B_{12}, and B_{66}, doubled the values when the thickness

doubled. Therefore, the minimization of the coupling effect, i.e., [B]≠0, seems to result from a combination of all factors listed above. In summary, the increase in the bending matrix components occurs at a much higher rate than that of the coupling matrix, and a decrease in extension-shear and bending-torsion coupling is also observed. From the manufacturing point of view, the tapering technique proposed by Tsai (2021) and employed by Vescovini et al. (2024) has proven to be a good option for reinforcing panels. However, the differences between modeling and experimental results remain under investigation.

The final stage of this section involves analyzing the bending/out-of-plane displacement of laminated plates. For this purpose, a simply supported rectangular plate (Lx = 180 mm and Ly = 900 mm, Ly Lx^{-1} = 5.0) was selected. The bending load applied is a uniform pressure of 1000 Pa for all cases, which serves as the lower bound for all scenarios. This bending uniform load is sufficient to cause a considerable out-of-plane displacement without inducing failure for the thinnest laminate (8 layers). The stacking sequences used in this analysis are outlined in Table 1.

By default, ANSYS ACP (the composite module) Workbench analysis for laminated composites can employ either solid or shell elements (Venkatesan et al., 2019). In this paper, the shell element was selected due to its greater computational efficiency. The present model consists of 1,729 nodes with a total of 10,374 degrees-of-freedom (Figure 1). The boundary conditions used were straightforward: the out-of-plane (typically the z-axis) displacements at all four edges were restricted, while all others were left free. To prevent rigid motion, two vertices were restricted—one in the x- and y-axes and the other in the y-axis only.

Table 2. Stiffness matrices for all cases.

Case	A_{ij} [N m^{-1}]x10^8	B_{ij} [N]x10^4	D_{ij} [N.m]
QUAD $[0/\pm 45/90]_s$	$\begin{bmatrix}0.52 & 0.16 & 0.00\\0.16 & 0.52 & 0.00\\0.00 & 0.00 & 0.18\end{bmatrix}$	$\begin{bmatrix}0.00 & 0.00 & 0.00\\0.00 & 0.00 & 0.00\\0.00 & 0.00 & 0.00\end{bmatrix}$	$\begin{bmatrix}7.17 & 1.10 & 0.44\\1.10 & 1.88 & 0.44\\0.44 & 0.44 & 1.30\end{bmatrix}$
DD $[\pm 18/\pm 62]_2$	$\begin{bmatrix}0.58 & 0.16 & 0.00\\0.16 & 0.43 & 0.00\\0.00 & 0.00 & 0.19\end{bmatrix}$	$\begin{bmatrix}-0.54 & 0.06 & -0.13\\0.06 & 0.43 & -0.12\\-0.13 & -0.12 & 0.06\end{bmatrix}$	$\begin{bmatrix}4.17 & 1.09 & 0.11\\1.09 & 3.18 & -0.12\\0.11 & -0.12 & 1.48\end{bmatrix}$
DD $[\pm 0/\pm 50]_2$	$\begin{bmatrix}0.76 & 0.15 & 0.00\\0.15 & 0.29 & 0.00\\0.00 & 0.00 & 0.18\end{bmatrix}$	$\begin{bmatrix}-0.58 & 0.16 & -0.07\\0.16 & 0.25 & -0.10\\-0.07 & -0.10 & 0.16\end{bmatrix}$	$\begin{bmatrix}5.52 & 1.12 & -0.08\\1.12 & 2.21 & -0.07\\-0.08 & -0.07 & 1.29\end{bmatrix}$
DD $[\pm 22.5/\pm 52.5]_2$	$\begin{bmatrix}0.53 & 0.18 & 0.00\\0.18 & 0.45 & 0.00\\0.00 & 0.00 & 0.21\end{bmatrix}$	$\begin{bmatrix}-0.47 & 0.03 & -0.14\\0.03 & 0.42 & -0.13\\-0.14 & -0.13 & 0.03\end{bmatrix}$	$\begin{bmatrix}3.84 & 1.25 & 0.11\\1.25 & 3.25 & -0.12\\0.11 & -0.12 & 1.65\end{bmatrix}$
QUAD $[0_3/\pm 45_2/90]_s$	$\begin{bmatrix}1.32 & 0.31 & 0.00\\0.31 & 0.72 & 0.00\\0.00 & 0.00 & 0.36\end{bmatrix}$	$\begin{bmatrix}0.00 & 0.00 & 0.00\\0.00 & 0.00 & 0.00\\0.00 & 0.00 & 0.00\end{bmatrix}$	$\begin{bmatrix}67.51 & 5.87 & 1.32\\5.87 & 10.72 & 1.32\\1.32 & 1.32 & 7.44\end{bmatrix}$
DD $[\pm 18/\pm 62]_4$	$\begin{bmatrix}1.17 & 0.32 & 0.00\\0.32 & 0.89 & 0.00\\0.00 & 0.00 & 0.37\end{bmatrix}$	$\begin{bmatrix}-1.08 & 0.11 & -0.25\\0.11 & 0.85 & 0.24\\-0.25 & 0.24 & 0.11\end{bmatrix}$	$\begin{bmatrix}37.55 & 10.26 & 0.22\\10.26 & 28.51 & -0.24\\0.22 & -0.24 & 12.19\end{bmatrix}$
DD $[\pm 0/\pm 50]_4$	$\begin{bmatrix}1.51 & 0.31 & 0.00\\0.31 & 0.58 & 0.00\\0.00 & 0.00 & 0.35\end{bmatrix}$	$\begin{bmatrix}-1.15 & 0.32 & -0.14\\0.32 & 0.50 & -0.20\\-0.14 & -0.20 & 0.32\end{bmatrix}$	$\begin{bmatrix}48.81 & 9.87 & -0.15\\9.87 & 18.67 & -0.14\\-0.15 & -0.14 & 11.40\end{bmatrix}$
DD $[\pm 22.5/\pm 52.5]_4$	$\begin{bmatrix}1.17 & 0.43 & 0.00\\0.31 & 0.67 & 0.00\\0.00 & 0.00 & 0.48\end{bmatrix}$	$\begin{bmatrix}-0.82 & 0.14 & -0.34\\0.14 & 0.54 & -0.25\\-0.34 & -0.25 & 0.14\end{bmatrix}$	$\begin{bmatrix}39.11 & 14.31 & 0.19\\14.31 & 22.23 & -0.45\\0.19 & -0.45 & 15.89\end{bmatrix}$
QUAD $[0/\pm 45/90]_{4s}$	$\begin{bmatrix}2.07 & 0.63 & 0.00\\0.63 & 2.07 & 0.00\\0.00 & 0.00 & 0.72\end{bmatrix}$	$\begin{bmatrix}0.00 & 0.00 & 0.00\\0.00 & 0.00 & 0.00\\0.00 & 0.00 & 0.00\end{bmatrix}$	$\begin{bmatrix}319.39 & 82.81 & 7.06\\82.81 & 234.66 & 7.06\\7.06 & 7.06 & 95.44\end{bmatrix}$
DD $[\pm 18/\pm 62]_8$	$\begin{bmatrix}2.34 & 0.65 & 0.00\\0.63 & 1.77 & 0.00\\0.00 & 0.00 & 0.74\end{bmatrix}$	$\begin{bmatrix}-2.16 & 0.22 & -0.50\\0.22 & 1.70 & -0.49\\-0.50 & -0.49 & 0.23\end{bmatrix}$	$\begin{bmatrix}308.73 & 85.01 & 0.44\\85.01 & 234.18 & -0.48\\0.44 & -0.48 & 98.35\end{bmatrix}$
DD $[\pm 0/\pm 50]_8$	$\begin{bmatrix}3.02 & 0.61 & 0.00\\0.63 & 1.15 & 0.00\\0.00 & 0.00 & 0.71\end{bmatrix}$	$\begin{bmatrix}-2.30 & 0.65 & -0.29\\0.65 & 1.01 & -0.41\\-029 & -0.41 & 0.65\end{bmatrix}$	$\begin{bmatrix}399.75 & 80.88 & -0.30\\80.88 & 152.73 & -0.28\\-0.30 & -0.28 & 93.38\end{bmatrix}$
DD $[\pm 22.5/\pm 52.5]_8$	$\begin{bmatrix}2.35 & 0.86 & 0.00\\0.86 & 1.33 & 0.00\\0.00 & 0.00 & 0.95\end{bmatrix}$	$\begin{bmatrix}-1.65 & 0.29 & -0.67\\0.29 & 1.08 & -0.50\\-0.67 & -0.50 & 0.29\end{bmatrix}$	$\begin{bmatrix}310.47 & 113.48 & 0.35\\113.48 & 176.61 & -0.41\\0.35 & -0.41 & 126.76\end{bmatrix}$

To enable a comparison between the finite element analysis and the analytical solution, the condition for a long composite plate must be enforced. As described in (Equation 18), this condition depends on the bending stiffness components (D_{11} and D_{22}). Another important consideration is the stress distribution through the thickness. The laminated plate stress analysis is based on the effective stress of the lamina (i.e., the sum of all plies) (Johri et al., 2022), enabling a fair comparison between different stacking sequences and thicknesses.

Table 3 summarizes the finite element results for all cases studied. As observed, as the number of repetitions increases, the DD performance improves. However, the angle selection appears to significantly impact the laminate plate bending performance. For thin (8 layers) and mid-thick (16 layers) laminates, the DD configuration for all three cases studied showed no improvement in either maximum out-of-plane displacement or effective stress when compared to the QUAD configuration. This phenomenon can be explained by the non-zero coupling stiffness matrix condition, which couples bending and extension, and the non-zero bending stiffness matrix components (D_{16} and D_{26}), which are responsible for twist-bending coupling.

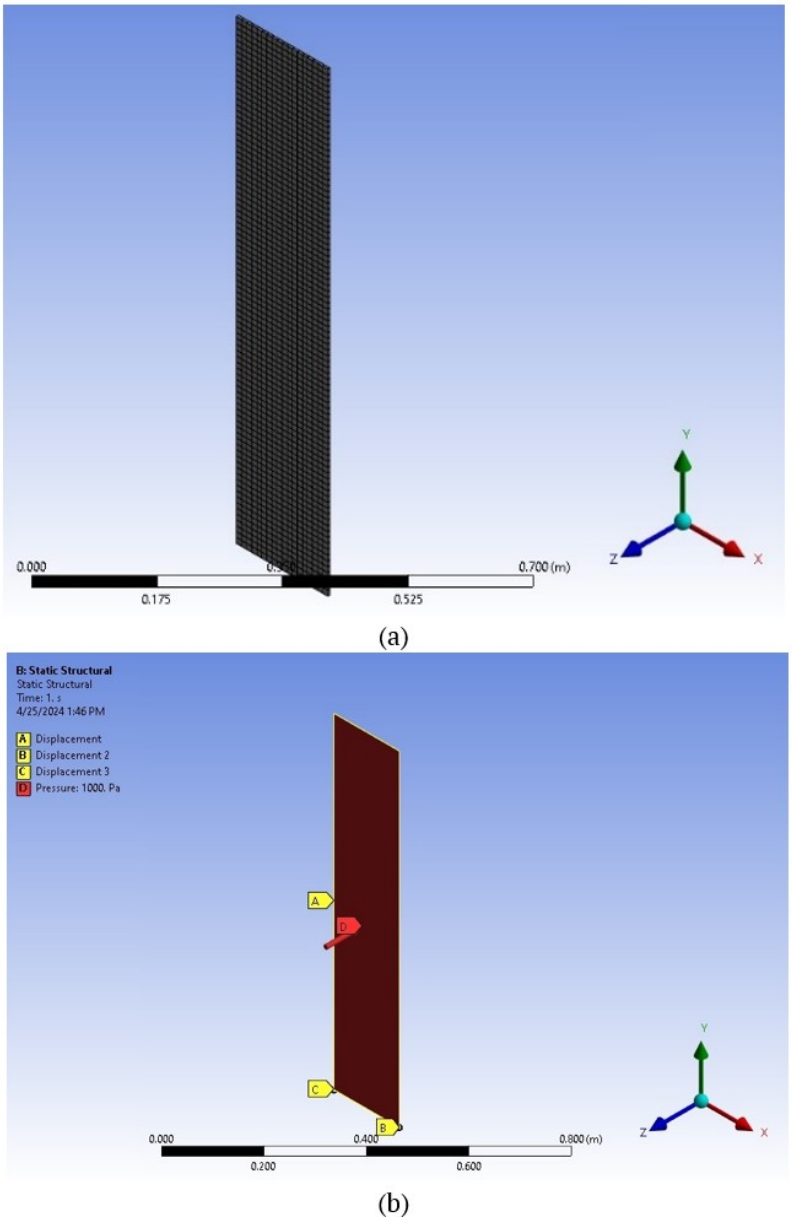

Figure 1. Finite element conditions. (a) Mesh; (b) Boundary conditions.

Table 3. Finite element results.

Case	Long plate condition [a.u]	Out-of-plane displacement [mm]		Equivalent stress [MPa]
		Analytical	Finite Element Method (FEM)	
QUAD $[0^o/\pm45^o/90^o]_s$	4.14	1.9058	1.8973	33.79
DD $[\pm18^o/\pm62^o]_2$	3.21	3.2740	3.2311	39.27
DD $[\pm0^o/\pm50^o]_2$	3.77	2.4746	2.4372	35.14

DD $[\pm 22.5^o/\pm 52.5^o]_2$	3.44	3.1916	3.1152	36.46
QUAD $[0_3^o/\pm 45_2^o/90^o]_s$	4.75	0.2025	0.2022	7.18
DD $[\pm 18^o/\pm 62^o]_4$	3.21	0.3640	0.3614	10.21
DD $[\pm 0^o/\pm 50^o]_4$	3.81	0.2800	0.2783	8.97
DD $[\pm 22.5^o/\pm 52.5^o]_4$	3.45	0.3607	0.3553	9.56
QUAD $[0^o/\pm 45^o/90^o]_{4s}$	3.24	0.0427	0.0428	3.03
DD $[\pm 18^o/\pm 62^o]_8$	3.21	0.0443	0.0442	2.66
DD $[\pm 0^o/\pm 50^o]_8$	3.81	0.0341	0.0343	2.31
DD $[\pm 22.5^o/\pm 52.5^o]_8$	3.45	0.0440	0.0437	2.49

For thick laminates (32 layers), a different scenario was observed. The effective stress for all three cases of DD configurations was on average 17.9% lower than the corresponding QUAD configuration. This can be partly explained by the QUAD configuration selected. The spatial distribution of 0°, ± 45°, and 90° layers through the thickness led to an increase in shear stress, thereby increasing the effective stress. The angular ply orientation for the DD configuration directly affected its bending stiffness and, consequently, the out-of-plane displacement.

Two DD configurations, namely $[\pm 18.0/\pm 62.0]_8$ and $[\pm 22.5/\pm 52.5]_8$, exhibited an increase in peak out-of-plane displacement of around 3.0%. The reason for such behavior is the decrease in the bending stiffness component D_{11}. The $[\pm 0.0/\pm 50.0]_8$ configuration showed the best performance regarding both effective stress and maximum out-of-plane displacement. This can be attributed to two factors: a large D_{11} and near-zero D_{16} and D_{26} components. Among all configurations tested, the DD $[\pm 0.0/\pm 50.0]_8$ configuration demonstrated the best performance for bending in thick composites, while for thin and mid-thick laminated composites, the QUAD configurations outperformed the equivalent DD stacking sequences. In conclusion, the overall performance of DD stacking sequences improves as the number of repetitions increases. Figure 2 illustrates the out-of-plane displacement distribution.

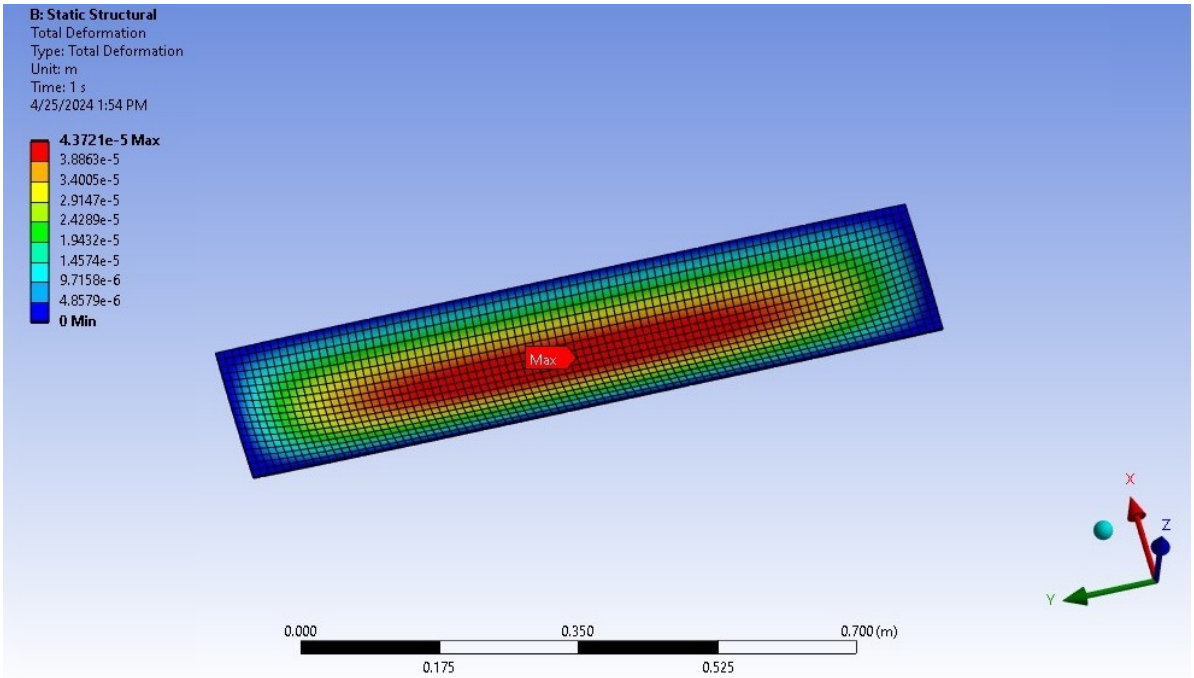

Figure 2. FEM results. Out-of-plane displacement distribution in meters.

Conclusion

A comparative study between two major groups of laminated composites stacking sequences, QUAD and the recent DOUBLE-DOUBLE, was performed. From the stiffness matrix point of view and under the Classical Laminate Theory, increasing the repetitions of the 4-layer sub-laminates [±Φ/±ψ] leads to an increase in bending stiffness at a much higher rate than the increase in coupling stiffness. At same time, it promotes a decrease in extension-bending (A_{16}, A_{26}) and bending-torsion (D_{16}, D_{26}) components.

The bending behavior of laminated plates using these two stacking sequences was investigated by the finite element method. The simulations, however, indicate that as the number of repetitions increases from two to eight, the out-of-plane displacement decreases when compared against the corresponding QUAD, making the DD configuration a good option. Angle selection also plays an important role in the overall bending behavior, as it affects three major components of the bending stiffness matrix: D_{11}, D_{16}, and D_{26}.

The best DD configuration for bending problems is $[\pm 0/\pm 50]_8$. The angle combination for the [± 0/± 50] sub-laminate led to a high value of D_{11} and near-zero D_{16} and $D_{26,}$ a combination that brings an increase in bending stiffness and a near-zero twist-bending coupling. The DD configurations seem to be a valuable option for bending applications in thick composites.

Acknowledgments

The authors express their gratitude for the logistical and financial support provided by the Mechanical Engineering Graduate Studies Program (PPGMEC) under the Coordination for the Improvement of Higher Education Personnel– (CAPES) grant 001. Additionally, the second author acknowledges the financial support provided by the Brazilian Research Council for Scientific and Technological Development – (CNPq) grant 307385/2022-1.

References

Arteiro, A., Sharma, N., Melo, J. D. D., Ha, S. K., Miravete, A., Miyano, Y., Massard, T., Shah, P. D., Roy, S., Rainsberger, R., Rother, K., Cimini Jr, C., Seng, J. M., Arakaki, F. K., Tay, T., Lee, W. I., Sihn, S., Springer, G. S., Roy, A., Riccio, A., & Hahn, H. T. (2020). A case for Tsai's modulus, an invariant-based approach to stiffness. *Composite Structures*, *252*, Artigo 112683. https://doi.org/10.1016/j.compstruct.2020.112683

Ávila, A. F., & Morais, D. T. S. (2009). Modeling nanoclay effects into laminates failure strength and porosity. *Composite Structures*, *87*(1), 55–62. https://doi.org/10.1016/j.compstruct.2007.12.009

Ávila, A. F., & Tamma, K. K. (1998). Analysis of laminate metal matrix composites. *Journal of Thermal Stresses*, *21*(8), 897–917. https://doi.org/10.1080/01495739808956183

Carley, G., Geraldo, V., De Oliveira, S., & Ávila, A. F. (2013). Nano-engineered composites: Interlayer carbon nanotubes effect. *Materials Research*, *16*(3), 628–634. https://doi.org/10.1590/S1516-14392013005000034

Falkowicz, K. (2021). Composite plate analysis made in an unsymmetric configuration. *Journal of Physics: Conference Series*, *2130*, Artigo 012014. https://doi.org/10.1088/1742-6596/2130/1/012014

Hart-Smith, L. J. (2004). Expanding the capabilities of the Ten-Percent Rule for predicting the strength of fibre-polymer composites. In S. W. Tsai (Ed.), *Failure criteria in fibre-reinforced-polymer composites* (pp. 597–642). Elsevier. https://doi.org/10.1016/B978-008044475-8/50021-4

Johri, N., Agarwal, G., Mishra, R. K., & Thakur, H. C. (2022). FEM analysis of polymeric hybrid composites. *Materials Today: Proceedings*, *57*, 383–390. https://doi.org/10.1016/j.matpr.2021.12.248

Kollar, L. P., & Springer, G. S. (2003). *Mechanics of composite structures*. Cambridge University Press.

Maji, A., & Mahato, P. K. (2022). Development and applications of shear deformation theories for laminated composite plates: An overview. *Journal of Thermoplastic Composite Materials*, *35*(11), 2576–2619. https://doi.org/10.1177/0892705720930765

Mantzaroudis, V. K., & Stamatelos, D. G. (2020). An approximate closed-form buckling solution for the local skin buckling of stiffened plates with omega stringers: The case of antisymmetric cross-ply and angle-ply laminations. *Structures*, *28*, 1196–1209. https://doi.org/10.1016/j.istruc.2020.09.035

Melo, J. D. D., Bi, J., & Tsai, S. W. (2017). A novel invariant-based design approach to carbon fiber reinforced laminates. *Composite Structures*, *159*, 44–52. https://doi.org/10.1016/j.compstruct.2016.09.055

Nimbolkar, P. V., & Jain, I. M. (2015). Cylindrical bending of elastic plates. *Procedia Materials Science*, *10*, 793–802. https://doi.org/10.1016/j.mspro.2015.08.001

O'Donnell, M. P., & Weaver, P. M. (2020). Reconsidering laminate nonsymmetry. *AIAA Journal*, *58*(4), 1811–1820. https://doi.org/10.2514/1.J058751

Paixão, N. M. M., & Ávila, A. F. (2023). Finite element simulations of auxetic structure combined with honeycomb using unidirectional continuous carbon fiber composite properties. *Journal of Engineering and Exact Sciences*, *9*(1), 15430–01e. https://doi.org/10.18540/jcecvl9iss1pp15430-01e

Patton, A., Antolín, P., Dufour, J. E., Sangalli, G., & Vázquez, R. (2021). Accurate equilibrium-based interlaminar stress recovery for isogeometric laminated composite Kirchhoff plates. *Composite Structures*, *256*, Artigo 112976. https://doi.org/10.1016/j.compstruct.2020.112976

Sheikhi, M., Rafiei Anamagh, M., Bediz, B., & Tunc, L. T. (2024). Design of manufacturable variable stiffness composite laminates using spectral Chebyshev and normalized cut segmentation methods. *Composite Structures*, *330*, Artigo 117836. https://doi.org/10.1016/j.compstruct.2023.117836

Shrivastava, S., Sharma, N., Tsai, S. W., & Mohite, P. M. (2020). D and DD-drop layup optimization of aircraft wing panels under multi-load case design environment. *Composite Structures*, *248*, Artigo 112518. https://doi.org/10.1016/j.compstruct.2020.112518

Singh, A., & Kumari, P. (2020). Analytical free vibration solution for angle-ply piezolaminated plate under cylindrical bending: A piezo-elasticity approach. *Advances in Computational Design*, *5*(1), 55–89. https://doi.org/10.12989/acd.2020.5.1.055

Tsai, S. W. (2021). Double–double: New family of composite laminates. *AIAA Journal*, *59*(10), 4293–4305. https://doi.org/10.2514/1.J060659

Venkatesan, K., Ramanathan, K., Vijayanandh, R., Raj Kumar, G., Jung, S., & Senthil Kumar, M. (2019). Comparative structural analysis of advanced multi-layer composite materials. *Materials Today: Proceedings*, *27*, 2673–2687. https://doi.org/10.1016/j.matpr.2019.11.247

Vermes, B., Tsai, S. W., Massard, T., Kim, H. J., & Scalici, T. (2021a). Design of laminates by a novel 'double–double' layup. *Thin-Walled Structures*, *165*, Artigo 107954. https://doi.org/10.1016/j.tws.2021.107954

Vermes, B., Tsai, S. W., Riccio, A., & Scalici, T. (2021b). Application of the Tsai's modulus and double-double concepts to the definition of a new affordable design approach for composite laminates. *Composite Structures*, *259*, Artigo 113246. https://doi.org/10.1016/j.compstruct.2020.113246

Vescovini, A., Li, C. X., Paz Mendez, J., & D'Ottavio, M. (2024). Post-buckling behavior and collapse of Double-Double composite single stringer specimens. *Composite Structures*, *327*, Artigo 117699. https://doi.org/10.1016/j.compstruct.2023.117699

Wang, Y., Wang, D., Zhong, Y., & Zhang, W. (2023). Topology optimization of Double-Double (DD) composite laminates considering stress control. *Computer Methods in Applied Mechanics and Engineering*, *414*, Artigo 116191. https://doi.org/10.1016/j.cma.2023.116191

Whitney, J. M. (1987). *Structural analysis of laminated anisotropic plates*. Technomic Publishing Company.

Yu, W. (2024). A review of modeling of composite structures. *Materials*, *17*(2), 446. https://doi.org/10.3390/ma17020446

Zhang, Z., Zhang, Z., Di Caprio, F., & Gu, G. X. (2022). Machine learning for accelerating the design process of double-double composite structures. *Composite Structures*, *285*, Artigo 115233. https://doi.org/10.1016/j.compstruct.2022.115233

Zhao, K., Kennedy, D., Miravete, A., & Scalici, T. (2023). Defining the design space for Double–Double laminates by considering homogenization criterion. *AIAA Journal*, *61*(7), 3190–3203. https://doi.org/10.2514/1.j062639